

A Study on Friction Materials for Brake Squeal Reduction by Nanotechnology

Masaaki Nishiwaki and Kenji Abe

Toyota Motor Corp.

Hikomichi Yanagihara and Igor Stankovic

Toyota Motor Europe NV/SA R&D.

Yuji Nagasawa

Toyota Central R&D Labs. Inc.

Satoshi Wakamatsu

ADVICS Co., Ltd.

Copyright © 2008 SAE International

ABSTRACT

Brake squeal is caused by dynamic instability, which is influenced by its dynamic unstable structure and small disturbance of friction force variation. Recently, FE Analysis of brake squeal is applied for brake design refinements, which is based on dynamic instability theory. As same as the refinement of brake structure is required for brake squeal reduction, the refinement of pad materials is also required for brake effectiveness and brake squeal reduction. It is well known that friction film, which is composed of polymers like phenol formaldehyde resin and so on, influences for friction coefficient. Therefore it is expected that the refinement of polymers in pad materials enable higher brake effectiveness and less brake squeal. In this paper, Molecular Dynamics is applied for the friction force variation of polymers in pad materials. The MD simulation results suggest the reduction method of friction force variation of polymers. The refinement of pad materials is shown here based on the MD simulation results, which is assured by experiments. This paper shows the possibility of friction materials design with higher performance and less brake squeal.

INTRODUCTION

Recently, higher brake performance including brake effectiveness is required for vehicle safety. At the same time, brake squeal reduction is also required for comfort. It is well known that pad materials of higher friction coefficient sometimes cause brake squeal generation. Brake noise reduction technology development [1] comes to be more important, because brake squeal is much influenced by friction coefficient of pad materials which is shown in references [2] and [3]. Brake squeal is

caused by dynamic instability of the vibration system composed of disc brake, knuckle and suspension. This is analyzed by flutter of the vibration system under small disturbance of friction force variation, which is shown in references [4] and [5]. Recently, FE Analysis of brake squeal [6] is applied for brake design refinements for brake squeal reduction. But it will be sometimes difficult to modify the vibration system for dynamic stability in all vibration modes. Then it will be more important to reduce brake friction force variation. This paper shows the concept of pad materials design for higher performance and less brake squeal, which is based on the MD simulation and experiment results.

INFLUENCES OF FRICTION SURFACE

Pad materials are composed of metal fiber, organic fiber, inorganic fiber, barite, other additives, graphite, phenol formaldehyde resin binder and organic fiber [7]. Table 1 shows the typical formulation of friction materials.

Table 1. Typical Formulation of Friction Materials

Material	Chemical Formula	Vol. %	Diameter (μm)	Density (g/cm^3)	Melting Point (°C)
Metal Fiber	Fe, Cu, etc.	10	< 200×3000	7~9	>1000
Organic Fiber	Aramid Pulp	10	~ 10×3000	1.4	>500(*d)
Inorganic Fiber	Mineral, Glass	10	< 10×3000	~4	~1000
Inorganic filler	Mineral, Glass	10	<200	~4	~1000
Barite	BaSO ₄	20	~10	4.5	1580
Other additives	Sulfide, Ca(OH) ₂	5	<200	~4	?
Graphite	C	5	<500	2.3	~3400
Organic Filler	Cashew Dust	10	~500	1.1	300~600(*d)
Phenolic Resin	(C ₆ H ₄ COCH ₂ O) _n	20	?	1.3	300~600(*d)

* decomposition

Figure 1 shows the friction surface between pad and disc. Friction force depends on the abrasive and adhesive friction mechanisms. Brake disc is composed

of cast iron. Throughout brake burnish, friction films including phenol formaldehyde resin are transferred from brake pads to disc surfaces. It is well known that friction coefficient μ is influenced by friction films shown in Figure 2, which is shown in references [8] and [9]. The friction force variation will be able to reduce with the refinement of polymers like phenol formaldehyde resin. In this paper, the higher friction coefficient pad material is applied for this experiment, which include low-steel fiber and 0.1% SiC abrasive. The higher stiffness and less damping pad material is applied for this experiment, which is removed of cashew dusts. The binder of pad materials is replaced of phenol formaldehyde resin to other polymers.

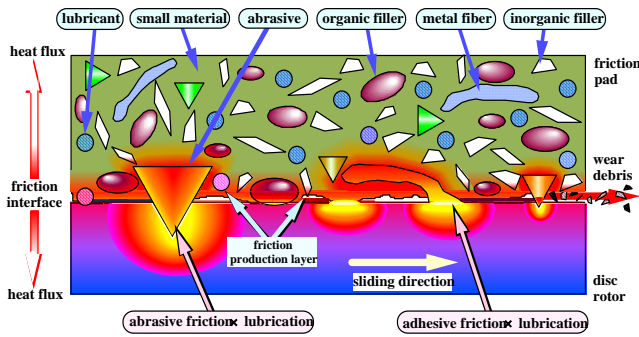


Figure 1. Friction Surfaces

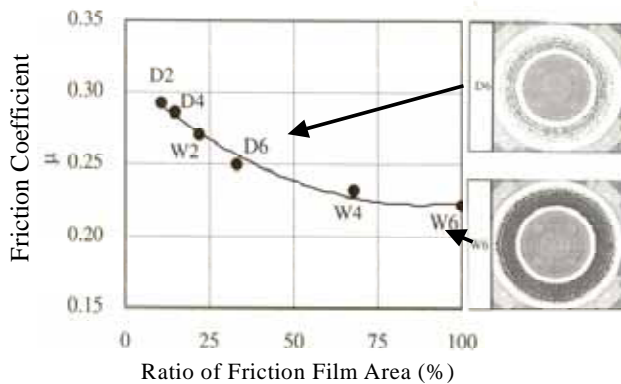


Figure 2. Influence of Friction Films [9]

REDUCTION OF FRICTION FORCE VARIATION IN POLYMERS

MODEL OF POLYMERS

It is known that the chemical constituents determine the factors in material behavior of macroscopic systems.

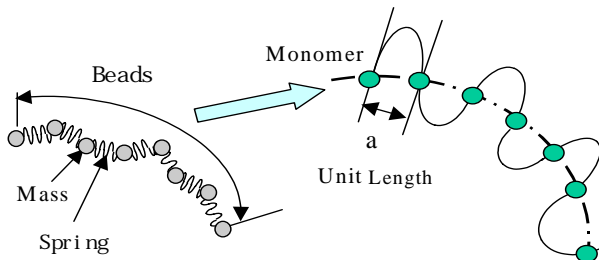


Figure 3. Models of Monomer and Polymer [10]

Figure 3 shows the monomer model of beads with masses and springs. Also Figure.3 shows the polymer model of a number of chemical units in coarse-grained model. A real polymer is assumed based on the model shown in reference [10]. Any measurable quantity Q with a dimension $[Q]$ specified in SI units kg, m and s, is made dimensionless by a reference quantity Q_{ref} in equation (1) for $[Q]$ in equation (2).

$$Q_{ref} = m^{+1/2} r_0^{+} s^{-1/2} \quad (1)$$

$$[Q] = \text{kg m s} \quad (2)$$

$$Q = Q_{dimless} Q_{ref} \quad (3)$$

The polymer chain length for linearity, the persistence length l_p determined by the chemical characteristics, is given by equation (4). The polymers come to get entangled for longer than l_p . On the other hand, the equation $l_p = 0$ represents no bending stiffness.

$$l_p = a (C + 1) / 2 \quad (4)$$

where a : Unit length shown in Figure 3 [10]
 C : Flory's coefficient

Table 2 shows the Q reference values of Poly-Tetra-Fluoro-Ethylene PTFE. The reference mass is calculated by the equation $m = m_b (l_p/l_p^*) / (\text{Avogadro constant})$. Unit mass standard polymer FENE model is shown in Table 4, which is derived from PTFE reference values. The reference values, length, energy and so on are calculated by the equations shown in Table 3.

Table 2. PTFE Reference Values

		PTFE reference value		PTFE reference value
mass	1 0 0	1.28×10^{-23} kg	shear rate	0 0 -1 2.1×10^{10} Hz
length	0 1 0	1.44×10^{-9} m	viscosity	1 -1 -1 1.9×10^{-4} Pas
time	0 0 1	4.77×10^{-11} s	temperature	1 2 -2 847.5 K
energy	1 2 -2	1.17×10^{-20} J	surface number density	0 -2 0 4800 cm^{-2}
force	1 1 -2	8.13×10^{-12} N	bulk mass density	1 -3 0 4.3 g/cm^3
stress	1 -1 -2	3.92×10^6 Pa	bulk number density	0 -3 0 3300 cm^{-3}

Table 3. Reference Values

Length	Number of Density	Temperature	Energy	Pressure	Time	Shear Rate
$l_{ref} = r_0$ $= l_p/l_p^*$	$n_{ref} = r_0^{-3}$	$T_{ref} = T_m/T_m^*$	$e_{0,ref} =$ $= k_B T_{ref}$	$P_{ref} =$ $= n_{ref} e_{0,ref}$	$t_{re} =$ $r_0 (m/e_{0,ref})^{1/2}$	$\dot{\gamma}_{ref} =$ t_{re}^{-1}

where k_B is Boltzmann constant and T_m is melting temperature in Kelvin

Table 4. Polymer Data

Polymer	FENE model	PTFE	PAI
Persistence length l_p (10^{-9} m)	1.34	19.3	35.0
Monomer weight m_b (g/mol)	1	626.2	190
Bond length a (10^{-9} m)	0.97	1.55	4.0
Characteristic ratio C	1.76	24.0	16.5
Critical weight N_c	100	21	
Melting temperature T_m (K)	0.7	593	548

The reference values can be calculated by equation (1). Then the stress of normal direction and shear stress in friction surface can be calculated in equations (1), (2) and (3). Friction coefficient is given by the ratio of normal and shear stresses.

DYNAMIC BEHAVIOR OF POLYMERS

Equation (5) gives the motion of mass m of bead, which is influenced by the potential U^{bond} composed of Leonard-Jones potential U^{LJ} and FENE model potential U^{FENE-C} shown in Figure.4. Based on the Molecular Dynamics theory, it is well known that potential function U^{bond} is governed by the distance of each mass r . The potential function U^{bond} is applied for this paper. Also equation (5) represents viscous-elastic characteristics of polymers. All entries for real polymers have been estimated from the reference [11]. The force represents the variation from initial value F_{int} throughout max value F_{max} to the final stable value.

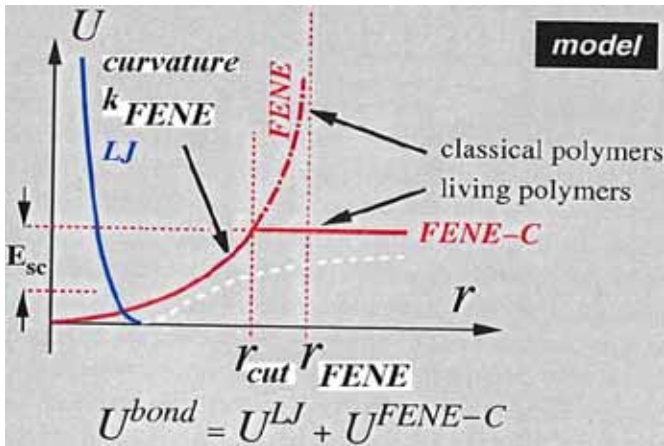


Figure 4. FENE Potential

$$M\ddot{x} = k_s(v_s t - x) - \dot{x} \dot{x} A - F_{max} - (F_{int} - F_{max})(1 - e^{-t/D}) \quad (5)$$

- where M : Monomer weight
- x : Displacement
- k_s : Spring stiffness
- \dot{x} : Derivative of Potential Function in Figure 4
- v_s : Shear rate
- t : time
- D : Damping factor
- A : Area
- F_{int} : Initial value of external force
- F_{max} : Maximum value of external force
- D : Aging time coefficient
- τ : Relaxation time coefficient

The speed of variation is determined by aging time coefficient D and relaxation time coefficient τ . Then the friction force variation can be calculated. Next step of the dynamic behavior of monomer is calculated by the last

calculation result. The dynamic behavior of monomer is predicted by the iteration of calculation. The friction coefficient μ is a dimensionless quantity which won't be influenced by inter molecular chemistry. Therefore one polymer is assumed by multi beads spring model with N_c beads in this calculation when FENE model has $N_c=100$ beads. Figure.5 shows the effect of aging for easy understanding. When the actual contact area is varied so quickly, friction force is also varied so quickly. Accordingly, friction force variation is influenced by aging time coefficient D and relaxation time coefficient τ . Friction force variation will be reduced by the refinements of parameters D and τ . Figure 6 shows the polymer model under shear force. It will be able to consider the reduction of stress concentration by the refinement of polymer and its characteristics.

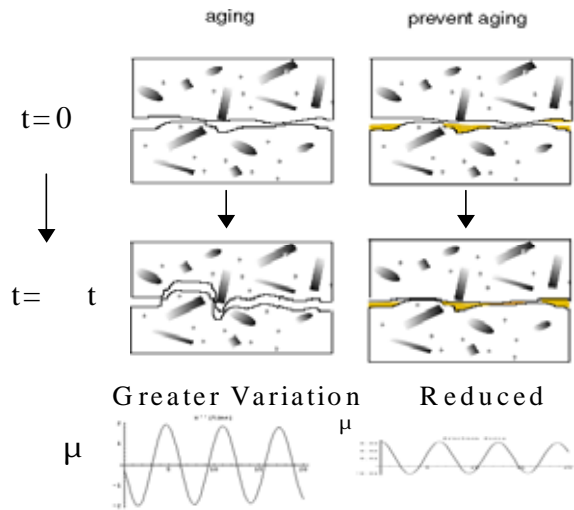


Figure 5. Friction Force Variation in Polymers

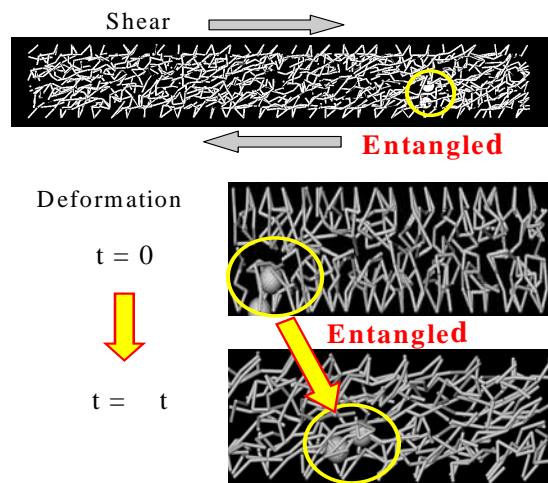
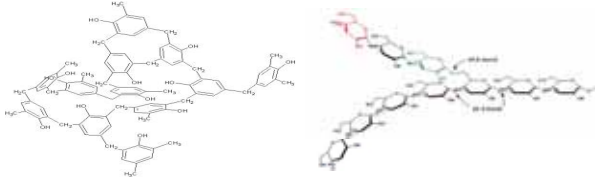


Figure 6. Polymers Model under Shear Force

The friction force variation become smaller in the polymer with straight chains type structure like Poly-Amid-Imides PAI than the polymer with 3-Dimensional chains type structure like Phenol formaldehyde resin. In case of the Phenol formaldehyde resin, double bond is presented by the chemical structure that gives higher friction coefficient and its variations. Its polymer chains structure can store amount of potential energy and its

polymer chains structure suddenly release its energy after yield stress. Then greater local variation of the shear stress and the normal stress cause the greater variation of friction coefficient [14].

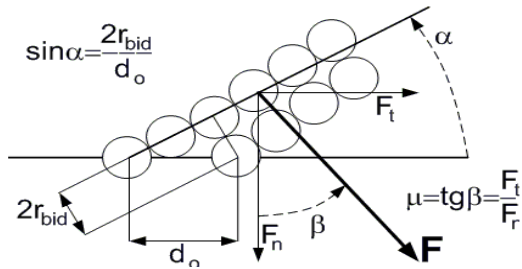


3-Dimensional chains type Straight chains

Figure 7. Molecular Structures [13]

CONSIDERATION OF DYNAMICS

The friction can be understood as a process of transfer of the energy from translation into normal motion of atoms. Friction coefficient μ depends on the equations (6), (7) and (8) shown in references [14] [15]. These equations are derived from each consideration of relationship between macroscopic and microscopic viewpoints. Figure 8 shows the polymer model located with the angles α and β to friction surface. The angle α gives the distance d_0 . Here $\mu = \tan \beta$ is assumed for the dependence on surface density, bead size, and polymer thickness in this model. Constant A is introduced to include the fact that non-zero friction exists, also when surface density is large and beads are very small. Equation (6) is given by the angle β in polymer friction surface and geometric factors r_{bid} , d_{surf} , d_0 and A of polymer model shown in Figure 8.



where

- $2 r_{bid}$: Diameter of Bead
- d_{surf}, d_0 : Distance between Each Bead
- α : Angle in Polymer and Friction Surface
- β : Angle in Force worked to Monomers

Figure 8. Polymers Model in Molecular Dynamics

$$\mu_1 = \frac{2 \frac{r_{bid}}{d_{surf}} + A}{\sqrt{1 - \left(2 \frac{r_{bid}}{d_{surf}}\right)^2}} \quad (6)$$

where A : Constant

Equation (7) is given by the ratio between viscous shear force and polymer diffusion force. When the diffusion constant D is very small through interface between disc and pad, Equation (7) has the value close to constant.

$$\mu_2 = \left(1 + \frac{6k_B TDL}{v}\right) \quad (7)$$

- where v : Velocity
- L : Polymer layer thickness
- T : Temperature
- k_B : Boltzmann constant
- D : Diffusion constant

Equation (8) is given by the entanglement of polymer length N_{bids} and FENE spring rigidity constants k_{FENE} [14], Here PTFE reference length l_{ref} is calculated by the equation $l_{ref} = [k_B (T_m/T_m) / (\text{yield stress})]^{1/3}$. In the yield stress 100Mpa of PTFE, $l_{ref} = 4.9/10^{10}$ [m] is calculated. Then Number of FENE Polymer for persistence length $N_{bids}-lp=19.3/4.9$ is calculated.

$$\mu_3 = \frac{1}{1 - \frac{C_N}{N_{bids}} - \frac{C_K}{k_{FENE}}} \quad (8)$$

- where C_N : Constant
- C_K : Constant
- $N_{bids} = lp/lp^*$
- lp^* : Persistence Length of FENE model
- k_{FENE} : Spring Rigidity of FENE model

Next, calculation results of friction coefficient based on the equations (8) are shown in Figure 9 and Figure 10. Parameter study was made in $N_{bids}-lp=4$ and $k_{FENE}=30$. FENE spring rigidity constant $k_{FENE}=30$ is assumed by the medium value of the general range of $k_{FENE}=5 - 60$. $N_{bids}-lp=4$ represents FENE model of PTFE, which represent the standard size for modeling. Polymer density N_{chain} is given by $N_{chain} = 8/r_{mon}$, where monomer thickness measured data divided by FENE length $r_{mon} = 5/4.9$. Figure 9 shows the friction coefficient μ influenced by polymer density N_{chain} and Number of FENE Polymer for persistence length $N_{bids}-lp$. In shorter $N_{bids}-lp$, μ become unstable with the variation of polymer density N_{chain} . In longer $N_{bids}-lp$, μ become stable for the variation of polymer density N_{chain} . Figure 9 shows the region suitable for higher friction coefficient μ and reducing its variation, which includes Poly-Amid-Imides PAI, Poly-Imides PI and Poly-Ether-Ether-Ketone PEEK. Figure 10 shows that the friction coefficient μ is influenced by polymer density N_{chain} and FENE spring rigidity constant k_{FENE} . In less k_{FENE} , μ become unstable with the variation of polymer density N_{chain} . In greater k_{FENE} , μ become stable with the variation of polymer density N_{chain} . Figure 10 shows the region suitable for higher friction coefficient μ and reducing its variation, which includes PAI. This region provides the reduction of

friction coefficient μ variation in higher temperature of friction surface.

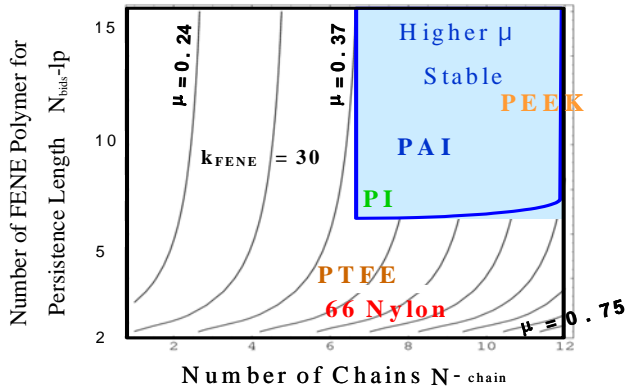


Figure 9. Friction Coefficient μ influenced by $N_{bids-lp}$ and N_{chain}

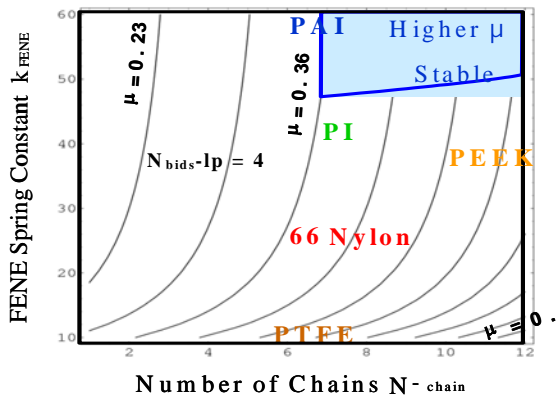


Figure 10. Friction Coefficient μ influenced by k_{FENE} and N_{bids}

Based on these considerations, the higher and stable friction coefficient μ requires three characteristics, polymer chains density $N_{chain} > 6$, Number of FENE Polymer for persistence length $N_{bids-lp} > 6$, FENE spring rigidity constants $k_{FENE} > 50$.

BRAKE SQUEAL MECHANISM

The dynamic instability theory [5] describes that flutter is caused by dynamic unstable structure of its vibration system and its small disturbance. The variation of friction coefficient μ in polymer was studied. The consideration of brake squeal mechanism is shown in Figure 11. The variation of friction coefficient μ is caused by aging of polymers, which is explained in Figure 5. Friction force variation between pad and disc causes the bending moment variation of disc shown in Figure 11. When its vibration mode is dynamic unstable, Brake squeal will be caused by flutter mechanism like coupled vibration of aircraft wings. Based on these considerations, the higher and stable friction coefficient μ is provided by the suitable polymers in the required regions in Figure 9 and Figure 10. The polymers are suitable for the pad materials in higher friction coefficient and less friction force variation for reducing brake squeal.

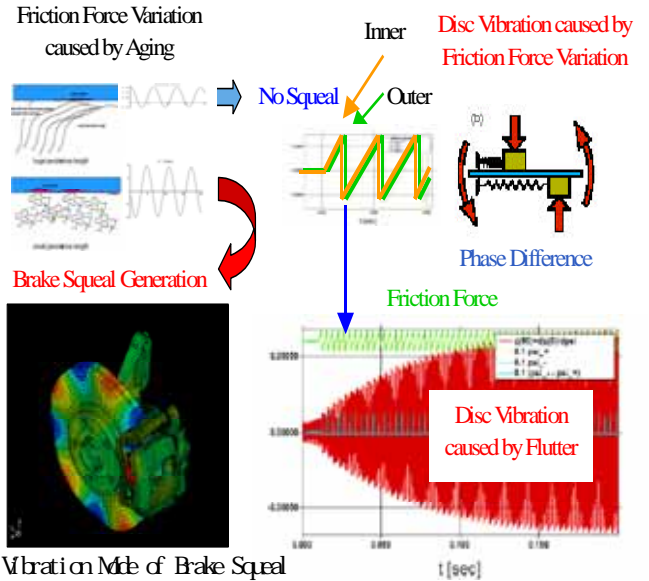


Figure 11. Brake Squeal Mechanism

EXPERIMENTS OF BRAKE SQUEAL

The variation of friction coefficient μ is reduced by the replacement of the 3-Dimensional chains type structure like Phenol formaldehyde resin to the other polymers with straight chains type structure like PAI. PI and PEEK. These considerations based on the calculation results shown in Figure 9 and Figure 10 were examined by some experiments of test peaces and full size disc brake.

FRICITION COEFFICIENT OF TEST PIECES

Figure 12 shows the friction coefficient measurement of test peaces [16]. This equipment is for $50 \times t5$ disc in cast iron, pad material 10×10 mm polymers or actual brake pad materials. The test peace is pushed against the disc by air cylinder controlled by load cell.

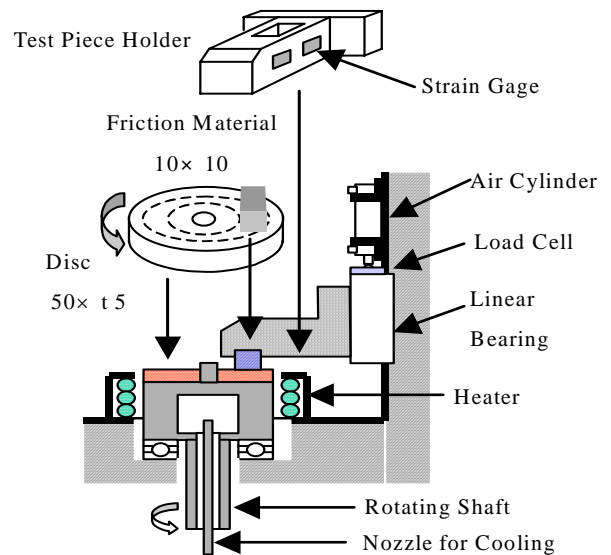


Figure 12. Friction Coefficient Measurement of Test Piece

Friction force is measured by strain gages. Then the friction coefficient is calculated by friction force, normal load and its geometry. Burnish was done under the conditions, normal load 200N, velocity 1m/s, temperature 75 or 150 and 1 hour. After burnish, the friction coefficient was measured under the condition, normal load 100N or 200N, velocity 1m/s 0 1m/s, temperature 75 or 150 .

TEST PIECES OF POLYMERS

It is predicted by calculation result shown in Figure 9 that the friction coefficient μ is stable in PAI, PI and PEEK. Figure 13 shows the experimental results. These graphs show the friction coefficient μ influenced by sliding velocity in Phenol formaldehyde resin, PAI and PEEK. The left graphs are for the pad temperature 75 . And the right graphs are for the pad temperature 150 . It is shown that the friction coefficient μ of Phenol formaldehyde resin is unstable, especially in 150 . On the other hand, the friction coefficient μ of PAI is stable. It is shown that the friction coefficient μ of PEEK is stable in 75 , but unstable in 150 . Figure 10 shows the influence of FENE spring rigidity constant k_{FENE} . It represents that the friction coefficient μ is influenced by FENE spring rigidity constant k_{FENE} , which represents the capacity for the influence of friction surface temperature. The friction coefficient μ is stable in higher FENE spring rigidity constant k_{FENE} .

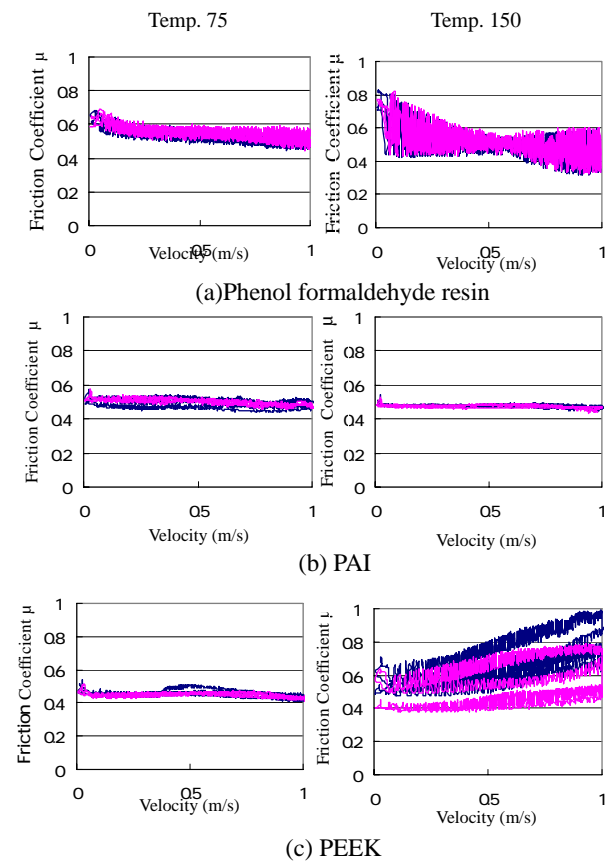


Figure 13. Friction Coefficient of Polymer Test Peaces

TEST PIECES OF PROTOTYPE MATERIALS

The higher friction coefficient pad material was applied for this experiment, which include low-steel fibber and 0.1% SiC abrasive. The higher stiffness and less damping factor pad material was applied for this experiment, which was removed of cashew dusts. And the binder of pad materials was replaced of Phenol formaldehyde resin to PAI. Figure 14 shows the friction coefficient in pad temperature 150 influenced by sliding velocity in conventional pad materials using Phenol formaldehyde resin binder and prototype pad materials using PAI binder.

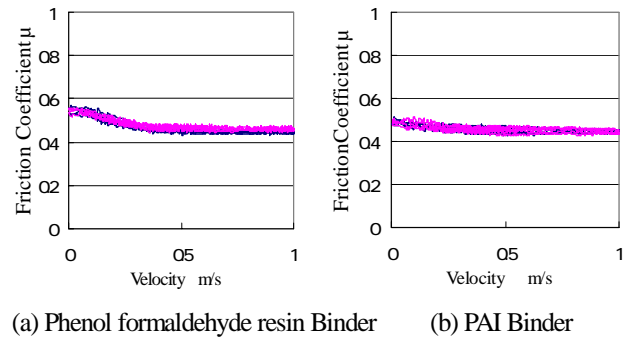


Figure 14. Friction Coefficients of Prototype Materials

The average μ is almost same. The negative slope of friction coefficient versus sliding velocity is a little bit different. It will be able to predict brake effectiveness. But it will be difficult to predict brake squeal generation based on the data in Figure 14. It is possible to predict brake squeal generation based on the data in Figure 13.

BRAKE NOISE TEST

Brake squeal evaluation tests were done by full size floating caliper front disc brake system for passenger car. This disc brake has 57 piston in cylinder of floating type caliper and 255 x 22mm ventilated type brake disc made of cast iron. Anti-squeal shims were removed for duplication of brake squeal test. Figure 15 and Figure 16 show the dynamometer brake squeal test results. Before brake squeal tests, 1000 times brake stops were done for brake burnish, which was constructed of initial vehicle velocity < 50 km/h, pad temperature <150 , desecration < 0.2g. After 1000 times brake burnish, 500 times stops were done for brake squeal evaluation test, which was constructed of the same kinds of braking condition. Figure 15 shows the comparison of the rate of brake squeal generation. The left graph, for the conventional pad material using Phenol formaldehyde resin binder, shows the rate of brake squeal 82% in 500 times braking. The right graph, for the prototype pad material using PAI binder, shows the rate of brake squeal 40% in 500 times braking. The friction coefficient is also measured in this brake squeal test. The average value of friction coefficient is almost same $\mu=0.42$. You can see the effect of the replacement of PAI binder.

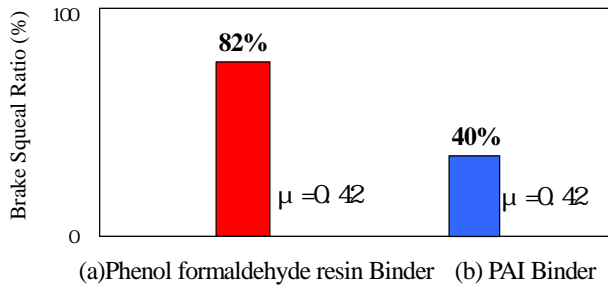


Figure 15. Ratio of Brake Squeal Generation

Figure 16 shows the comparison of the brake squeal frequency and sound pressure level. When brake squeal occur, its peak of sound pressure and squeal frequency analyzed by FFT was plotted in Figure 16. The left graph is for the conventional pad material, and the right graph is for the prototype pad material. The sound pressure level is reduced 20 dB lower. Then brake squeal was almost disappeared.

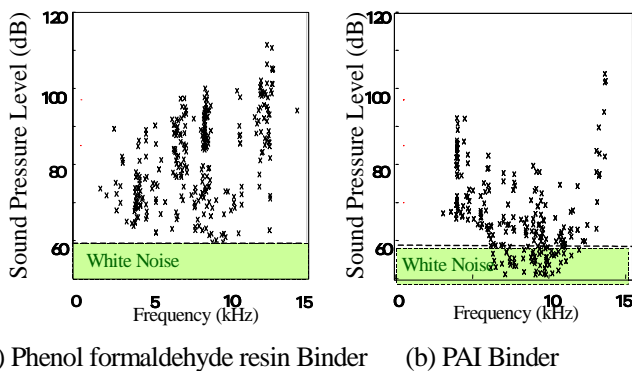


Figure 16. Brake Squeal Evaluation Tests

This replacement of polymer provides the same level brake effectiveness and the remarkable brake squeal reduction. Based on the consideration of polymer friction force variation, prototype pad material was designed for higher friction coefficient and less brake squeal.

CONCLUDING REMARKS

- (1) Brake Squeal is caused by dynamic instability, which depends on its dynamic unstable structure of vibration system and its disturbance of friction force variation. As same as brake structure refinement for dynamic stability is required for no brake squeal, the reduction of friction force variation is also required.
- (2) This paper shows the possibility of higher brake performance with less brake squeal in pad materials design. The higher friction coefficient μ and the reduction of its variation can be provided by the replacement of straight chain type molecule structure polymers.

- (3) The higher friction coefficient μ and the reduction of its variation can be provided by the three suitable characteristics, polymer chains density $N_{\text{chain}} > 6$, Number of FENE Polymer for persistence length $N_{\text{bids-lp}} > 6$, FENE spring rigidity constants $k_{\text{FENE}} > 50$. The refined pad material products will be developed after other requirements studies, fade, wear, and so on.

REFERENCES

1. M.Nishiwaki, "Review of study on brake squeal", Japan Society of Automobile Engineering Review, 11(4), p.48-54 (1990).
2. N. Millner, "An Analysis of Disc Brake Squeal", SAE Paper, 780332 (1978)
3. M.Erikson and S.Jacobsen, "Friction behavior and squeal generation of disc brake at low speed, Proc. Instn. Mech. Engrs., Part D, Journal of Automobile Engineering, p.1245-1256(2001)
4. M.Nishiwaki, "Generalized Theory of Brake Noise", Proc. Inst. Mech. Engrs., Journal of Automobile Engineering, Vol.207, Part D, p195-202 (1993).
5. V.V.Bolotin, " Nonconservative Problems of the Theory of Elastic Stability", Pergamon Press, p.7-9 (1963).
6. G.D.Liles, "Analysis of Disc Brake Squeal Using Finite Element Methods", SAE Paper, 891150 (1989).
7. Y.Sasaki and S.Kusaka, "The Transition of Automotive Brake Lining Materials", Journal of Japanese Society of Tribologists, Vol.41, NO.4, p.197-201 (2003)
8. S.K.Rhee, M.G.Jacko and H.S.Tsang, "The role of friction film in friction, wear and noise of automobile brakes", SAE Paper No.900004 (1990).
9. N.Odani, M.Kobayashi and K.Kakahara, " Effect of Transferred Surface Film on μ Behavior of Disc Brake Pad in Humidity Environment", SAE Paper No. 1991-01-3391(1991).
10. H.Yanagihara and M.Kroeger, "Polymer material design method and design system", Japan Patent Application Number 2005-163662 (2005).
11. R.S.Porter and J.F.Johnson, Chem. Rev.66, 1(1966); J.Brandrup and E.H.Immergut (eds), Polymer Handbook, Wiley-Interscience, New York, 2nd ed., (1975)
12. M.Kroeger, "Simple models for complex non equilibrium fluids", Physics Reports p.453-551 (2004)
13. Wikipedia, the free encyclopedia, "Phenol formaldehyderesin", <http://en.wikipedia.org/wiki/Phenol>
14. M.Nishiwaki, H.Yanagihara, Y.Fujioka, K.Abe and H.Isono, "Design method of friction materials with no noise", Patent pending.
15. J.Kim, "Atomic-scale origins of friction", langmuir, 12, p.4564-4566 (1996).
16. Y.Nagasawa, K.Yoshida, M.Hashimoto and M.Nishiwaki, "Friction test piece tester, Japan, Patent Application Number 2004-12172 (2004).